ACS OMEGA

Open Access

http://pubs.acs.org/journal/acsodf

Article

Effect of Polyethylene Pyrolysis Oil Hydrotreatment on the Pt/Al_2O_3 Catalyst: Experimental Characterization

Panayiota Adamou, Eleana Harkou, Ali Bumajdad, Xander De Jong, Maarten Van Haute, Achilleas Constantinou,* and Sultan Majed Al-Salem*

Cite This: *ACS Omega* 2024, 9, 19057−19062

Read Online

ACCESS | Metrics & More | Article Recommendations | Supporting Information

ABSTRACT: The dramatic increase in plastics production, coupled with a low recycling and recovery rate, has been a major challenge for sustainable practices and combating climate change. Hydrotreatment processing to upgrade fuel oils is a well-known process in the petroleum industry. In this work, we aim to investigate the catalyst properties before and after the hydrotreatment of pyrolysis oil derived from plastics, namely, linear low-density polyethylene, as no such report is available in the literature. Granular and powder forms of the Pt/Al_2O_3 catalyst were used in this study with characterization methods executed as such: transmission electron microscopy, X-ray photoelectron spectroscopy (XPS), X-ray diffraction (XRD), thermogravimetric analysis (TGA), and IR-RIS. XRD data show that the crystallinity of the catalyst support was unaffected by the hydrotreatment without any residues left, as the characteristic diffraction peaks were indicated for the crystalline phase of the support as 37.4, 39.8, 46.3, and 67.3°. In addition, the TGA experiments revealed that the carbon deposition on the spent catalyst was higher, as indicated by the higher weight loss (15.359%) compared to the fresh catalyst sample (11.43%). XPS analysis showed that the carbon deposition is more intense on the granular spent catalyst, as the intensity of the peaks is some 15 times greater than the peaks from the fresh catalyst. Also, compared to the observed peaks of the powder catalyst, less coke is formed. The band at 1624.05 cm^{-1} from the IR-RIS spectra was attributed to a shifted C═O band from the coke formation. The extension of these investigations using different catalysts to improve their characteristics and performance and to inhibit coke deposition will contribute to the incorporation of such processes in industry as well as the cost of fuels.

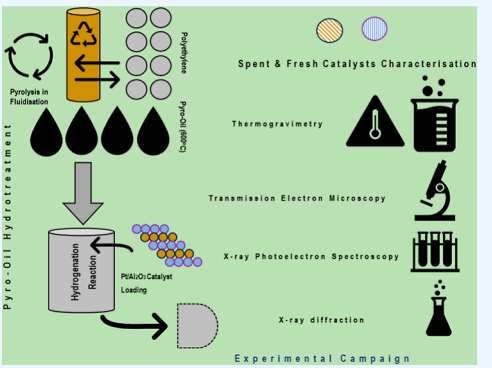

1. INTRODUCTION

The annual production of plastics has drastically increased, with an estimate to reach 500 million tonnes in 2025.[1] A mere 9% of the generated plastic waste (PW) is recycled, which increases its unsanitary landfill disposal.[2,3] Thermochemical technologies, namely pyrolysis,[4] received renewed attention due to the fact that the conversion of feedstock is carried out in the absence of oxygen, eliminating the generation of toxic gas emissions.[5] Moreover, studies indicate that pyrolysis has an economic advantage once environmental impact and scale are considered.[6,7] High-density polyethylene underwent pyrolysis at 250−400 °C, achieving 98.12% conversion at 350 °C by Ahmad et al.[8] Liquid products (80.88%) were analyzed using FTIR and GC−MS, revealing a composition rich in naphtha hydrocarbons, primarily in the gasoline (C6−C12: 32.56%) and diesel range (C13−C16; 30.8%). The hydrocarbon distribution showed 59.70% paraffinic, 31.90% olefinic, and 8.40% naphthenic.

PE was subjected to noncatalytic and thermally catalytic degradation at 450 °C using ultrastable Y (USY) zeolite by Kassargy et al.[9] Noncatalytic pyrolysis produced 80% wax, while catalytic pyrolysis yielded 71% liquid products with minimal coke deposition. The liquid fraction (C5−C39) required separation for future use as gasoline and diesel-like fuels. Optimal separation at 170 °C aligned with diesel and gasoline fuel characteristics. Postseparation, the diesel-like fuel constituted 35.3% with a high cetane number (53), and the gasoline-like fuel, 57%, exhibited a high-octane number (RON = 97). Both studies concluded that liquid fractions met the fuel grade requirements, indicating potential applications.

Oils derived from the pyrolysis of biomass have been proven for their potential as a high-end fuel through the process of hydrotreatment.[10,11] Hydrotreatment aims to reduce O_2 content and catalytically increase the stability and calorific value of the pyro-oil. Hydrotreatment is a well-established process in the petroleum industry and was employed on oils derived from biomass in the past,[12] with no research

Received: December 6, 2023
Revised: March 29, 2024
Accepted: April 2, 2024
Published: April 16, 2024

conducted as of yet on its effect on the catalyst used post-treatment of PW pyrolysis oil.[13] The development of efficient hydrogenation catalysts to promote the process is considered to be a key factor.[14] Noble and transition metals are most commonly used for upgrading pyrolysis oils,[15] but there is no literature that reports the changes occurring due to the process of upgrading pyrolysis oil. In this study, hydrotreatment of the pyrolysis oil derived from pilot-plant studies on polyethylene was conducted in a batch reactor using a 1 wt % Pt/Al_2O_3 catalyst. The oil was derived at an average operating temperature of 600 °C from a fluidized bed reactor (FBR),[16,17] and the oil was upgraded through hydrotreatment with the aim of experimentally studying the catalyst's properties.[18] To the best of our knowledge, no such report is available in the literature as the one presented in this communication for the effect of hydrotreatment on the catalyst used in plastic pyrolysis oil hydrotreatment.

2. EXPERIMENTAL SECTION

Linear low-density polyethylene pyrolysis took place using a FBR, as depicted elsewhere, to simulate one of PW's common components,[16] and the pyro-oil used for this study was extracted at 600 °C. Details of the process parameters were provided earlier by our research group.[17,18] The hydrotreatment process took place using a 500 mL Premex system-batch reactor equipped with an impeller for mixing gases into the liquid phase, as detailed in the Supporting Information (Figure S1). Further details on hydrotreatment are provided elsewhere.[19] The catalysts used were prepared by a dry impregnation method.[18] Al_2O_3 support (spheres) was impregnated with chloroplatinic acid salt solution ($H_2PtCl_6{\cdot}6H_2O$), and the catalyst was then reduced under H_2 flow using 1.75 g of Pt/Al_2O_3 with a mixture of pyro-oil and heptane (Figure S1). Impregnation of 15 g of Al_2O_3 in spherical form (1.8 mm Al_2O_3 spheres with a surface area of 200−220 m^2/g) (Sasol Co.), was conducted with chloroplatinic acid solution (chloroplatinic acid hexahydrate) as indicated in our past work.[18,19] The support used was $H_2PtCl_6{\cdot}6H_2O$ (Sigma-Aldrich/Merck product number: 206083) to obtain as close to 1.0 wt % Pt on the support as possible.[19] Approximately 0.4016 g of the chloroplatinic acid salt was used to perform the dry impregnation using 11 mL of demi-water. After the dry impregnation method was used, the catalyst was dried at 110 °C for 7 h in an atmosphere of air and calcined at 350 °C for 4 h.[18] Later, the catalyst was reduced under a flow of 33% hydrogen and 67% nitrogen under 16 bar pressure and at 250 °C for 3 h.[18,19] Granular and powder catalysts (after grinding) were used in this work, focusing on fresh and spent specimens. A series of experiments were performed for the characterization of fresh and spent catalysts to satisfy this study's objective. First, a pestle and mortar were used to granulate the fresh and spent catalyst specimens (>20 nm), as detected by transmission electron microscopy (TEM) conducted using a 120 kV JEM-1400 Flash (JEOL) system. X-ray photoelectron spectroscopy (XPS) and X-ray diffraction (XRD) studies were also conducted. The XPS spectra were recorded using an ESCALAB 250i (Thermo Scientific, UK) using Al K_α monochromatic radiation (1486.6 eV) with a spot size of 850 μm and processed with Thermo Avantage software (version 5.956). The XRD pattern, however, was studied using a Siemens/Bruker D 5000 diffractometer (USA). The quantification of coke deposited was determined by thermogravimetric analysis (TGA) measuring weight loss. The FTIR-6300 spectrometer (PerkinElmer Spectrum 2/3) was used for the IR study. Further experimental details depicting each technique and protocol used are provided in Table S1.

3. RESULTS AND DISCUSSION

3.1. X-ray Diffraction. XRD data for the fresh and spent catalysts are depicted in Figure S2. It was observed that the catalyst displays similar XRD patterns in both sizes, with prominent characteristic diffraction peaks (37.4, 39.8, 46.3, and 67.3°) revealing the presence of a crystalline phase for the Al_2O_3 support and Pt species (39.8, 46.3, and 67.3°). Moreover, it was observed that the strong diffraction peaks at 2θ angles of 46 and 67°, which were assigned to γ-Al_2O, were overlapping the diffraction peaks observed for Al_2O_3 support and Pt metallic species, revealing that the support of the catalyst is the γ-Al_2O_3 structure. This is confirmed by the broadening of the peaks.[20] There is no notable difference between fresh and spent catalyst samples, indicating coke formation on the support. This could be attributed to the sensitivity of the results, as XRD patterns do not show a peak for metals up to 15% of the loaded weight,[21] and the fact that Pt is impregnated deeper than 5 nm (i.e., the detection limit of the XRD instrument), which is not an indicator for coke formation. Also, the peak intensities between fresh and spent catalysts were similar, indicating that the crystallinity of the support was not affected and that there were no residues from the reaction.[21] Coke formation is discussed hereafter in the next sections using data extracted from different instrumentation.

3.2. Thermogravimetry. TGA was used to quantify the carbon formation over the spent powder form catalyst. Both catalysts were exposed and subjected to N_2 from room temperature to 1000 °C, and the results are presented and compared in Figure S3. The highest weight loss of 15.359% appears on the spent catalyst due to the carbon deposition, while the fresh catalyst showed a weight loss of 11.43%. This indicates that some 4% is attributed to carbon deposition on the spent catalyst. Also, similar studies showed that the coke deposition is formed on the surface of Pt particles,[22] which is verified by TGA and XRD profiles. The fact that the XRD data of fresh and spent catalysts were similar shows that the crystallinity of the support was not affected, and herein there was no coke deposition on the support. Since conventional catalysts (e.g., Pt/Al_2O_3) show rapid deactivation, coke formation catalyst clogging, and sintering, the development of nanomaterials is a promising technology to upgrade them.[23] Gholizadeh et al.[12] also reported the effect of hydrogen and bio-oil inlet temperatures on coke formation in order to inhibit and minimize the coking and the deactivation of the catalyst.

3.3. X-ray Photoelectron Spectroscopy. *3.3.1. Granular Catalyst.* XPS analysis was used to investigate the chemical composition of the catalyst, and the survey scan conducted is shown in Figure S4, identifying elements present on the surface of the catalyst. The catalysts consisted of Pt (barely detectable), C, Al, and O. Dai et al.[24] confirmed this phenomena, showing that Pt possesses weak absorption intensity due to its typically low content present on surfaces. Also, an overlap between the Al 2p and Pt 4f lines was observed, which was attributed to the similar binding energies of both components causing an overlap and disruption of the XPS signal. Additional peaks labeled as C KL and O KL are representative of the energy of the Auger electrons. This

https://doi.org/10.1021/acsomega.3c09729
ACS Omega 2024, 9, 19057−19062

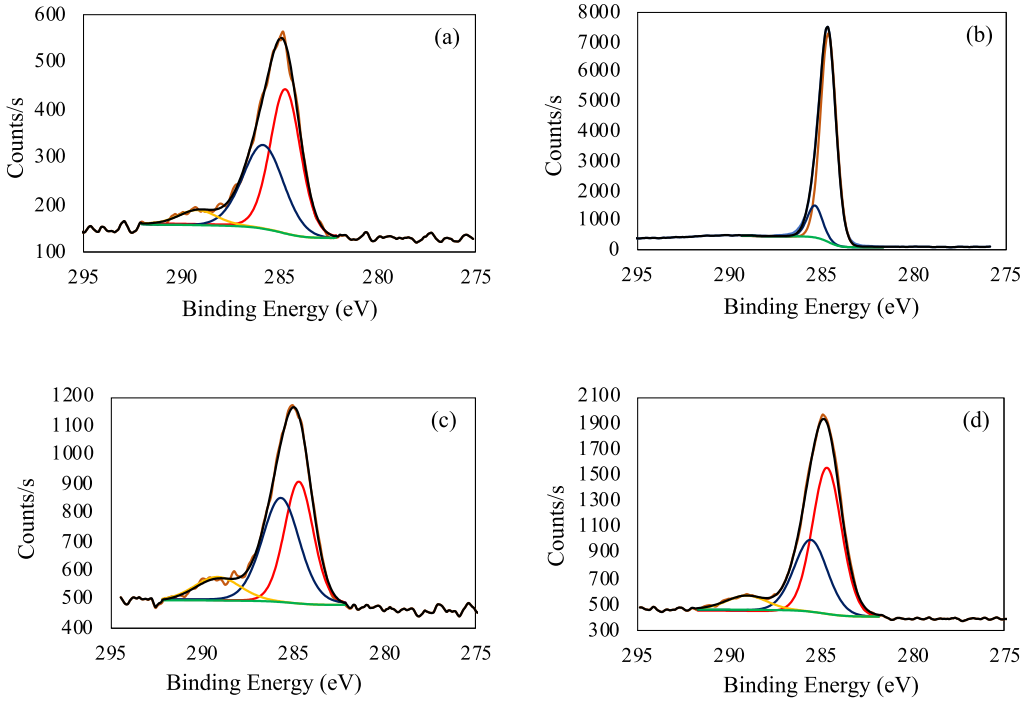

Figure 1. XPS spectra of (a) C 1s in fresh granular form, (b) C 1s in spent granular form, (c) C 1s in fresh powder form, and (d) C 1s in spent powder form.

process occurs when an electron from the K shell is ejected and an L-level electron drops to fill the empty vacancy, coupled with the ejection of an electron from the L shell.[25] Figure S4 also depicts the C 1s high resolution of the spectrum. The peak at 284.69 eV is a standard value of the binding energy for the chemical bond C−C. The characteristic peak at 285.81 eV is a result of the bond between C and O; the minor peak at 289.16 eV might be a result of species with a C═O bond.[26] XPS analysis was also conducted for O 1s, Al 2p, Pt 4d, and Pt 4f. A typical peak at 531.44 eV is attributed to Al_2O_3 and at 532.80 eV, which is a characteristic peak for C−O bond (Figure S4). Figure S4b illustrates the Al 2p XPS spectra, where the presence of an Al oxide peak at 74.76 eV agrees with the oxide state of the alumina. The standard value for metallic Pt is 71.0 eV; however, a shift to the left in the XPS peak was notable. The approximate value of 74 eV is related to its oxidation state corresponding to a higher shift in the binding energy.

XPS was also conducted on the spent catalyst to evaluate its surface after hydrotreatment. From the survey scan (Figure S5), it is evident that the components on the surface of the catalyst are the same as the fresh one, but the atomic ratio of C compared to the fresh catalyst is higher. This can be explained by the coke formation that resulted after the hydrotreatment. The deposition of carbonaceous substances occurs on the surface, decreasing the pore size and blocking the access to the active sites.[27] Figure 1 shows that the C 1s and C 1s peaks are slightly shifted to 284.60 and 285.33 eV, respectively. Oxygen-containing C species with single bond are still present in the spent catalytic surface after the hydrotreatment. The intensity of the peaks is almost 15 times higher in the spent catalyst, confirming C-containing compounds deposit on the surface of the material. The high-resolution spectrum of the O 1s does not differentiate from the fresh catalyst except for the intensity that is two times lower in the spent catalyst (Figure S5a). The same was observed for the XPS analysis of Al 2p and Pt 4f (Figure S5b,c); the peaks remained the same, but the intensity is three times lower; meaning that less of these elements are on the surface of the catalyst. Tables S2 and S3 illustrate the values of the surface elemental composition for both the fresh and spent samples.

3.3.2. Powder Catalyst. XPS analysis was also conducted on the powder catalyst (Figure S6), showing similar results to the granular catalyst, with the exception that Cl was detectable on the surface. This could be attributed to the chloroplatinic acid salt used for preparing the catalyst, which is available on the surface of the catalyst in its powder form. It is noteworthy that the intensity is one order higher in all the XPS spectra of the powder catalyst when compared to the granules, meaning that there are more elements on the (bigger) surface area in the powder form.[28] The peaks from C 1s high-resolution spectra are typical for carbon-based species and are the same as the granular form but with higher intensity (Figure 1c below). Figure S6 also shows the spectra of Al and Pt, respectively, which is in agreement with the data from the fresh sample of the granular form with higher intensity. Chlorine species were found on the surface with a peak of 199.19 eV, belonging to inorganic chlorine. Similarly, the presence of Cl could be attributed to the chloroplatinic acid salt used for catalyst preparation. From the survey scan shown in Figure S7f, it is observed that on the surface of the catalyst there are no Cl elements; when compared with the granular form, the intensity of C did not significantly increase. This indicates that not much coke was formed on this form of catalyst. Figure 1d depicts the C 1s spectra and confirms the previous observation compared with the granular form, in which the intensity of C did not increase much while compiled with the TGA results. That is also evident, from Figure S7 for O 1s, Al 2p, and Pt 4f, respectively, with a minor decrease in intensity. Tables S4 and S5 depict the elemental composition of the species on the surface for both fresh and spent samples.

https://doi.org/10.1021/acsomega.3c09729
ACS Omega 2024, 9, 19057−19062

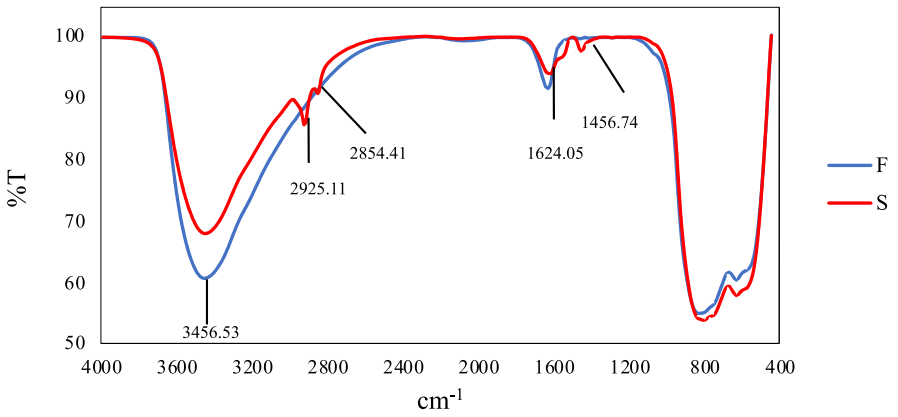

Figure 2. FTIR spectra (transmission, %) of the fresh (F) and spent (S) powder form of the Pt/Al_2O_3 catalyst.

3.4. InfraRed Spectroscopy. The Fourier-transform infrared spectra (FT-IR spectra) of the fresh and spent catalysts are shown in Figure 2. The spinel structure of γ-Al_2O_3 is well-known to occur over a range of hydrogen content, which is represented by the empirical formula $H_{3m}Al_{2-m}O_3$, thus the broad, rounded peak observed at 3456.53 cm^{-1} corresponds to the hydrogen bond between hydroxyl groups in γ-Al_2O_3 particles.[29] The band at 1638.62 cm^{-1} belongs to the bending mode of water, while the bands at 834.88 and 635.94 cm^{-1} are attributed to a metal−oxygen bond and, in that case, an Al−O bond from the alumina support. The peak at 635.94 cm^{-1} can be assigned to the AlO_6 stretching mode, while at 834.88 cm^{-1} relates to the AlO_4 stretching mode, indicating that γ-Al_2O_3 has both tetrahedral and octahedral coordination.[30] The IR spectra for the spent sample vary from the fresh one. The bands at 2925.11 and 2854.41 cm^{-1} correspond to C−H stretching vibrations, while the peak at 1456.74 cm^{-1} could be attributed to C−C stretching and C−H scissoring.[31] The band at 1624.05 cm^{-1} corresponds to C═C stretching or a shifted C═O band, resulting from coke formation. A shift can be observed for the band at 810.41 cm^{-1} (834.88 cm^{-1} at the fresh sample), indicating a stronger Al−O bond.

3.5. Transmission Electron Microscopy. TEM analysis was conducted for the powder catalyst since it exhibited better catalytic activity and it was not possible to do analysis on the granular form. As seen from the TEM analysis of the fresh sample (Figure S8), γ-Al_2O_3 displays a rod-like nanostructure with a maximum length of 20 nm.[32,33] Pt/γ-Al_2O_3 TEM analysis presents well-distributed Pt particles over the alumina surface with a particle size of 20 nm.[34,35] In our case, only a few Pt particles are shown on the surface of the support. This agrees with the XRD analysis that Pt is deeply impregnated within the porous material and is not available on the outside surface of the support. The spent catalyst presents minor differences compared to the fresh sample. The TEM images show a few morphological changes of the spent catalyst due to the agglomeration of metal particles at high temperatures. This causes a slight irregularity in the metal's distribution across the alumina support. It is evident that there is a slight coke formation, as confirmed by XPS and TGA analysis. Since the coke deposition occurs on Pt particles, there is not much carbon on the support.

4. CONCLUSIONS

In this work, the effect of hydrotreatment on a Pt/Al_2O_3 catalyst was studied using pyrolysis oil derived from polyethylene. The catalyst was used in two forms; granular and powder form and different characterization techniques were utilized on fresh and spent samples of both forms of catalyst. XRD results showed no difference between fresh and spent samples, but it confirmed the presence of γ-Al_2O_3 and Pt particles with characteristic peaks of 37.4, 39.8, and 67.3 and 39.8, 46.3, and 67.3° respectively. TGA analysis was performed for the quantification of carbon formed during hydrotreatment on the powder form catalyst. The results revealed a weight loss of 15.359% in the spent catalyst due to carbon deposition on the Pt species. XPS analysis was conducted in both forms of Pt/Al_2O_3. The spent catalyst of the granular form showed a 15-fold increase of the atomic ratio of the carbon compared with the fresh sample, indicating coke formation on the surface of the catalyst. This was also confirmed by the peaks observed which were 284.6 and 285.33 eV. In contrast, in the spent powder form, there was not a significant rise in the intensity of carbon, suggesting that there are fewer active sites occupied by carbonaceous species since there is a greater surface area in the powder form. Moreover, the peak for C 1s slightly changed from 284.65 to 284.64 eV. The FT-IR spectra also reveal peaks in the spent sample that were not present in the fresh and correspond to saturated and unsaturated carbon species, such as 2925.11 and 2854.41 cm^{-1} for C−H and 1624.05 cm^{-1} for C═C and C═O bonds. Lastly, TEM analysis was performed on the powder samples. Fresh samples revealed a rod-like structure of 20 nm length for γ-Al_2O_3 and few Pt species on the surface since they are deep-impregnated in the porous material. Minor changes were observed, confirming the results from XPS and TGA that there is only a slight coke formation in the powder form. Therefore, hydrotreatment has a different effect based on the form of catalyst used.

■ ASSOCIATED CONTENT

Supporting Information

The Supporting Information is available free of charge at https://pubs.acs.org/doi/10.1021/acsomega.3c09729.

Detailed experimental plan and results obtained in this communication (PDF)

https://doi.org/10.1021/acsomega.3c09729
ACS Omega 2024, 9, 19057−19062

AUTHOR INFORMATION

Corresponding Authors

Achilleas Constantinou − *Department of Chemical Engineering, Cyprus University of Technology, 3036 Limassol, Cyprus*; Email: a.konstantinou@cut.ac.cy

Sultan Majed Al-Salem − *Environment & Life Sciences Research Centre, Kuwait Institute for Scientific Research (KISR), 13109 Safat, Kuwait*; orcid.org/0000-0003-0652-4502; Email: ssalem@kisr.edu.kw

Authors

Panayiota Adamou − *Department of Chemical Engineering, Cyprus University of Technology, 3036 Limassol, Cyprus*

Eleana Harkou − *Department of Chemical Engineering, Cyprus University of Technology, 3036 Limassol, Cyprus*

Ali Bumajdad − *Department of Chemistry, Faculty of Science, Kuwait University, 13060 Safat, Kuwait*; orcid.org/0000-0003-2978-0103

Xander De Jong − *Q8 Research, Kuwait Petroleum Research and Technology B.V., 3198 LS Europoort Rotterdam, Netherlands*

Maarten Van Haute − *Q8 Research, Kuwait Petroleum Research and Technology B.V., 3198 LS Europoort Rotterdam, Netherlands*

Complete contact information is available at: https://pubs.acs.org/10.1021/acsomega.3c09729

Author Contributions

P.A.: data analysis and initial and final draft preparation; E.H.: data analysis and initial and final draft preparation; A.B.: experimental analysis and initial and final draft preparation; X. De J.: experimental analysis and final draft preparation; M. van H.: final draft review; A.C.: conceptualization, data analysis, and initial and final draft preparation; S.M. Al.-S.: conceptualization, data analysis, and initial and final draft preparation.

Notes

The authors declare no competing financial interest.

ACKNOWLEDGMENTS

The project leader would like to acknowledge the Kuwait Foundation for the Advancement of Sciences (KFAS) and the Kuwait Institute for Scientific Research (KISR) for initially funding grant EM114C (AP21-45 EC-01), which this work extends from, in collaboration with Kuwait Petroleum Research and Technology (KPRT—Q8 Research) and Kuwait University's (KUniv) general facilities projects GS 01/01, GS 01/05, GS 03/01, and the Science Nanoscopy Centre at the Faculty of Science.

REFERENCES

(1) Zhang, F.; Zhao, Y.; Wang, D.; Yan, M.; Zhang, J.; Zhang, P.; Ding, T.; Chen, L.; Chen, C. Current technologies for plastic waste treatment: A review. *J. Clean. Prod.* **2021**, *282*, 124523.

(2) Chawla, S.; Varghese, B. S.; A, C.; Hussain, C. G.; Keçili, R.; Hussain, C. M. Environmental impacts of post-consumer plastic wastes: Treatment technologies towards eco-sustainability and circular economy. *Chemosphere* **2022**, *308*, 135867.

(3) Evode, N.; Qamar, S. A.; Bilal, M.; Barceló, D.; Iqbal, H. M. N. Plastic waste and its management strategies for environmental sustainability. *Case Stud. Chem. Environ. Eng.* **2021**, *4*, 100142.

(4) Armenise, S.; SyieLuing, W.; Ramírez-Velásquez, J. M.; Launay, F.; Wuebben, D.; Ngadi, N.; Rams, J.; Muñoz, M. Plastic waste recycling via pyrolysis: A bibliometric survey and literature review. *J. Anal. Appl. Pyrolysis* **2021**, *158*, 105265.

(5) Dai, L.; Zhou, N.; Lv, Y.; Cheng, Y.; Wang, Y.; Liu, Y.; Cobb, K.; Chen, P.; Lei, H.; Ruan, R. Pyrolysis technology for plastic waste recycling: A state-of-the-art review. *Prog. Energy Combust. Sci.* **2022**, *93*, 101021.

(6) Fivga, A.; Dimitriou, I. Pyrolysis of plastic waste for production of heavy fuel substitute: A techno-economic assessment. *Energy* **2018**, *149*, 865−874.

(7) Yadav, G.; Singh, A.; Dutta, A.; Uekert, T.; DesVeaux, J. S.; Nicholson, S. R.; Tan, E. C.; Mukarakate, C.; Schaidle, J. A.; Wrasman, C. J.; et al. Techno-economic analysis and life cycle assessment for catalytic fast pyrolysis of mixed plastic waste. *Energy Environ. Sci.* **2023**, *16*, 3638−3653.

(8) Ahmad, I.; Khan, M. I.; Khan, H.; Ishaq, M.; Tariq, R.; Gul, K.; Ahmad, W. Pyrolysis Study of Polypropylene and Polyethylene Into Premium Oil Products. *Int. J. Green Energy* **2015**, *12* (7), 663−671.

(9) Kassargy, C.; Awad, S.; Burnens, G.; Kahine, K.; Tazerout, M. Experimental study of catalytic pyrolysis of polyethylene and polypropylene over USY zeolite and separation to gasoline and diesel-like fuels. *J. Anal. Appl. Pyrolysis* **2017**, *127*, 31−37.

(10) Cheah, Y. W.; Salam, M. A.; Sebastian, J.; Ghosh, S.; Arora, P.; Öhrman, O.; Olsson, L.; Creaser, D. Upgrading of triglycerides, pyrolysis oil, and lignin over metal sulfide catalysts: A review on the reaction mechanism, kinetics, and catalyst deactivation. *J. Environ. Chem. Eng.* **2023**, *11* (3), 109614.

(11) Lv, D.-C.; Jiang, K.; Li, K.; Liu, Y.-Q.; Wang, D.; Ye, Y.-Y. Effective suppression of coke formation with lignin-derived oil during the upgrading of pyrolysis oils. *Biomass Bioenergy* **2022**, *159*, 106425.

(12) Gholizadeh, M.; Gunawan, R.; Hu, X.; Kadarwati, S.; Westerhof, R.; Chaiwat, W.; Hasan, M. M.; Li, C. Z. Importance of hydrogen and bio-oil inlet temperature during the hydrotreatment of bio-oil. *Fuel Process. Technol.* **2016**, *150*, 132−140.

(13) Han, Y.; Gholizadeh, M.; Tran, C. C.; Kaliaguine, S.; Li, C. Z.; Olarte, M.; Garcia-Perez, M. Hydrotreatment of pyrolysis bio-oil: A review. *Fuel Process. Technol.* **2019**, *195*, 106140.

(14) He, Y.; Liu, R.; Yellezuome, D.; Peng, W.; Tabatabaei, M. Upgrading of biomass-derived bio-oil via catalytic hydrogenation with Rh and Pd catalysts. *Renewable Energy* **2022**, *184*, 487−497.

(15) Zhao, C.; Hong, C.; Hu, J.; Xing, Y.; Ling, W.; Zhang, B.; Wang, Y.; Feng, L. Upgrading technologies and catalytic mechanisms for heteroatomic compounds from bio-oil − A review. *Fuel* **2023**, *333*, 126388. Feb

(16) Al-Salem, S.; Van Haute, M.; Karam, H. J.; Hakeem, A.; Meuldermans, W.; Patel, J.; Hafeez, S.; Manos, G.; Constantinou, A. Fuel Range Properties of Oil and Wax Obtained from Catalytic Pyrolysis of Linear Low-Density Polyethylene in a Fluidized Bed Reactor (FBR). *Ind. Eng. Chem. Res.* **2022**, *61* (43), 16383−16392.

(17) Hafeez, S.; Van Haute, M.; Constantinou, A.; Al-Salem, S. M. Process Simulation Modeling of the Linear Low-Density Polyethylene Catalytic Pyrolysis in a Fluidized Bed Reactor. *Ind. Eng. Chem. Res.* **2023**, *62* (16), 6386−6393.

(18) Hafeez, S.; Van Haute, M.; Manos, G.; Karam, H. J.; Constantinou, A.; Al-Salem, S. M. Hydrotreatment over the Pt/Al2O3 Catalyst of Polyethylene-Derived Pyrolysis Oil and Wax. *Energy Fuels* **2023**, *37* (20), 16181−16185.

(19) Al-Salem, S. M.; Van Haute, M.; Constantinou, A.; et al. *Investigating the Effect of Different Mixtures of Plastic Solid Waste Feedstock on Pyro-Products, Final Report*; Egeria Nifaia Project Code: EM114C, 2023.

(20) Yatsenko, D. A.; Pakharukova, V. P.; Tsybulya, S. V. Low temperature transitional aluminas: structure specifics and related x-ray diffraction features. *Crystals* **2021**, *11* (6), 690.

(21) Al-Iessa, M. S.; Al-Zaidi, B. Y.; Almukhtar, R. S.; Shakor, Z. M.; Hamawand, I. Optimization of Polypropylene Waste Recycling Products as Alternative Fuels through Non-Catalytic Thermal and Catalytic Hydrocracking Using Fresh and Spent Pt/Al2O3 and NiMo/Al2O3 Catalysts. *Energies* **2023**, *16* (13), 4871.

https://doi.org/10.1021/acsomega.3c09729
ACS Omega 2024, 9, 19057−19062

(22) Alvarez-Galvan, M. C.; Navarro, R. M.; Rosa, F.; Briceño, Y.; Ridao, M. A.; Fierro, J. L. G. Hydrogen production for fuel cell by oxidative reforming of diesel surrogate: Influence of ceria and/or lanthana over the activity of Pt/Al2O3 catalysts. *Fuel* **2008**, *87* (12), 2502−2511.
(23) Shahbeik, H.; Shafizadeh, A.; Gupta, V. K.; Lam, S. S.; Rastegari, H.; Peng, W.; Pan, J.; Tabatabaei, M.; Aghbashlo, M. Using nanocatalysts to upgrade pyrolysis bio-oil: A critical review. *J. Clean. Prod.* **2023**, *413*, 137473.
(24) Dai, P.; Zhao, X.; Xu, D.; Wang, C.; Tao, X.; Liu, X.; Gao, J. Preparation, characterization, and properties of Pt/Al2O3/cordierite monolith catalyst for hydrogen generation from hydrolysis of sodium borohydride in a flow reactor. *Int. J. Hydrogen Energy* **2019**, *44* (53), 28463−28470.
(25) Zhang, S.; Li, L.; Kumar, A. *Materials Characterization Techniques*; CRC Press, 2008.
(26) Morgan, D. J. Comments on the XPS analysis of carbon materials. *C* **2021**, *7* (3), 51.
(27) Rodríguez, E.; Félix, G.; Ancheyta, J.; Trejo, F. Modeling of hydrotreating catalyst deactivation for heavy oil hydrocarbons. *Fuel* **2018**, *225*, 118−133.
(28) He, L.; Fan, Y.; Bellettre, J.; Yue, J.; Luo, L. A review on catalytic methane combustion at low temperatures: Catalysts, mechanisms, reaction conditions and reactor designs. *Renew. Sustain. Energy Rev.* **2020**, *119*, 109589.
(29) Hosseini, S. A.; Niaei, A.; Salari, D. Production of γ-Al₂O₃ from Kaolin. *Open J. Phys. Chem.* **2011**, *01* (02), 23−27.
(30) Siahpoosh, S. M.; Salahi, E.; Hessari, F. A.; Mobasherpour, I. Facile synthesis of γ-alumina nanoparticles via the sol-gel method in presence of various solvents. *Sigma J. Eng. Nat. Sci.* **2017**, *35* (3), 441−456.
(31) Omwoyo, J. B.; Kimilu, R. K.; Onyari, J. M. Catalytic pyrolysis and composition evaluation of tire pyrolysis oil. *Chem. Eng. Commun.* **2023**, *210* (7), 1086−1096.
(32) Abdollahifar, M. Synthesis and characterisation of γ-Al2O3 with porous structure and nanorod morphology. *J. Chem. Res.* **2014**, *38* (3), 154−158.
(33) Samain, L.; Jaworski, A.; Edén, M.; Ladd, D. M.; Seo, D. K.; Javier Garcia-Garcia, F.; Häussermann, U. Structural analysis of highly porous γ-Al2O3. *J. Solid State Chem.* **2014**, *217*, 1−8.
(34) Christoglou, C.; Alphonse, P.; Armand, C.; Desnoyer, C.; Vahlas, C. Complex Pt/Al2O3 materials for small catalytic systems. *Surf. Coat. Technol.* **2007**, *201* (22−23), 9195−9199.
(35) Usman, M. R.; Cresswell, D. L.; Garforth, A. A. Methylcyclohexene and Methylcyclohexadiene Dehydrogenation−Hydrogenation over Pt/Al 2 O 3 Catalyst. *Arabian J. Sci. Eng.* **2021**, *46*, 6635−6643.

https://doi.org/10.1021/acsomega.3c09729
ACS Omega 2024, 9, 19057−19062